Estimating Orion Heat Shield Failure Due To Ablator Cracking During The EFT-1 Mission

Jeremy C. Vander Kam[1]
NASA Ames Research Center, Moffett Field, CA, 94086 USA

Peter Gage[2]
Neerim Corp., Mountain View, CA, 94086, USA

The Orion EFT-1 heatshield suffered from two major certification challenges: First, the mechanical properties used in design were not evident in the flight hardware and second, the flight article itself cracked during fabrication. The combination of these events motivated the Orion Program to pursue an engineering-level Probabilistic Risk Assessment (PRA) as part of heatshield certification rationale. The PRA provided loss of Mission (LOM) likelihoods considering the probability of a crack occurring during the mission and the likelihood of subsequent structure over-temperature. The methods and input data for the PRA are presented along with a discussion of the test data used to anchor the results. The Orion program accepted an EFT-1 Loss of Vehicle (LOV) risk of 1-in-160,000 due to in-mission Avcoat cracking based on the results of this analysis. Conservatisms in the result, along with future considerations for Exploration Missions (EM) are also addressed.

Nomenclature

∞	=	Infinity
CDF	=	Cumulative probability Density Function
CTE	=	Coefficient of Thermal Expansion
E(n)	=	Young's Modulus as a function of parameter *n*
EFT-1	=	Exploration Flight Test 1
F.S./FoS	=	*Factor of Safety*
f(n)	=	Function of the parameter, *n*
FEM	=	Finite Element Model
GN&C	=	Guidance, Navigation, and Control
H/CG	=	Honeycomb, Gunned
k_{PFEM}	=	Finite Element Model-derived stress factor for pressure loads
k_{TFEM}	=	Finite Element Model-derived stress factor for temperature loads
LOM	=	Loss of Mission
LOV	=	Loss of Vehicle
M.S.	=	Margin of Safety
P	=	Pressure
P(n)	=	Probability of event *n*
PDF	=	Probability Density Function
T	=	Temperature
t	=	Time
ΔT	=	Temperature Change
μ	=	Mean
σ	=	Standard Deviation
σ_{app}	=	Applied Stress

[1] Deputy Orion TPS System Manager, NASA ARC, MS 258-1 Moffett Field CA, 94035, AIAA Senior Member
[2] Principal, Neerim Corp., NASA Research Park MS 19-46A Moffett Field CA 94035-0001, AIAA Senior Member

I. Introduction

THE essential function of any Thermal Protection System (TPS) is to limit the peak temperature of the spacecraft structure and systems to acceptable levels during atmospheric entry. More specific lower-level requirements are generally derived from this high level requirement, and their aggregate verification constitutes verification of the essential function. Within the lower requirements set, structural requirements on the thermal protection material itself and the attachment of the material to underlying structure are often imposed to assure that entry heating does not have a direct path to the primary structure and that the TPS material remains attached.

For the Orion EFT-1 heatshield, there was a derived requirement for positive structural margin against cracks extending through the thickness of the Avcoat thermal protection material. Prior to heatshield fabrication, the Program predicted positive B-basis margins against the Avcoat strength allowables developed to date. After the flight heatshield had been built, witness panels indicated that the mechanical properties used in design were not evident in the flight hardware. When these as-built strength allowables were used, negative B-basis margins were predicted for some of the design load cases. Furthermore, the flight article itself cracked at some of the honeycomb seams during fabrication. The seams were repaired, but the strength of the repairs was not well characterized and the as-built strength of the un-cracked seams was unknown.

The combination of these events motivated the Orion Program to pursue an engineering-level Probabilistic Risk Assessment (PRA) as part of the Heat Shield certification rationale for the EFT-1 flight. The key to this analysis is recognition that a crack is not itself a failure, but instead a potential initiator for structural over-temperature and subsequent failure. The failure sequence is summarized in equation 1. Loss Of Mission (LOM) as a consequence of cracking occurs only if the bondline below the crack is heated above its allowable temperature and if the elevated temperature weakens the underlying structure to the extent that applied load exceeds its reduced strength.

$$P\left(LOM_{crack}\right) = P\left(crack\right) \cdot P\left(overtemperature\right) \cdot P\left(structural failure\right) \tag{1}$$

A second crack-induced failure mode is when peel stresses adjacent to the foot of the crack cause failure of the bond between TPS and substrate. For EFT-1, structural analysis showed positive margins against peel so it was not included in the PRA assessment, nor is it included in this paper.

Section II provides a general discussion of the Orion structural design requirements and their implied reliability requirements. It will be shown that the reliability of a structure with positive margin per design policy far exceeds the reliability requirement levied on the TPS, which was 1/5300 for an ISS-type mission at the completion of system Preliminary Design Review [2]. The level of reliability depends on both the variability of possible loading and variability of material strength and is not always well controlled by classical structural design policy approaches, as will be discussed.

Section III presents the specific EFT-1 Loss of Vehicle (LOV) likelihood assessment due to the failure mode expressed in Equation 1 used for EFT-1 flight rationale. A simple approach is used to estimate an upper bound on failure probability, consistent with guidance in NASA's Risk Management Procedures [1], which notes:

"If uncertainty can be shown to be small based on a simplified analysis… then detailed uncertainty analysis is unnecessary."

The predicted probability of overheating, based on the first two terms in Equation 1, is sufficiently low that the third term, which addresses the likelihood of structural failure given that it is overheated, receives only cursory discussion. More refined analysis of this term would not influence a EFT-1 flight readiness decision.

II. Reliability Associated with Positive Structural Margin

The structural design policy for the Orion program largely follows NASA STD 5001B [3] for Factor of Safety, NASA STD 5002 [4] for Loads, and NASA STD 6016 [5] for material allowables. Structures are required to have a positive Margin of Safety (M.S.), as specified in Equation 2:

$$M.S. = \frac{AllowableLoad}{AppliedLoad \cdot FactorofSafety} - 1 \tag{2}$$

Generally, an A-basis allowable load is required, which means that 99% of the material samples used to determine material strength exceed the design value, with 95% confidence. Assuming a normal Gaussian distribution, this corresponds to a 2.33 "sigma" design level – or a value 2.33 standard deviations less than the mean value.

If a material has yield behavior, as for metals, margins may be written against both yield strength and ultimate strength. Here we will consider yield margins with a Factor of Safety of 1.0 on limit load and ultimate margins with a factor of safety of 1.4 on limit load.

NASA STD 5002 defines limit load as follows:

"*The maximum anticipated load experienced by a structure during a loading event, load regime, or mission.* ***Uncertainty factors associated with model uncertainty or forcing function uncertainty shall be incorporated into the limit load as reported." (emphasis added)***

While there is no statistical requirement for addressing load variability, it is common to perform a Monte Carlo study with a loads model to generate a range of load cases. For the Orion heatshield, for example, input parameters for the entry loads analysis, such as velocity and vehicle attitude, were varied throughout their range of statistical values, and resultant loads were calculated. A value at the upper end of the calculated range is selected as the limit load for the system. Often a statistical curve, such as the normal Gaussian distribution, is fit to the loads results and a value three standard deviations (or 3-sigma) above the mean is used as the limit load. This is not the maximum possible load, but a level at which only 1/741 missions would be expected to experience a higher load (and it is unlikely that even those missions would see much higher load).

It is now possible to estimate a lower bound on reliability that is delivered by satisfying the structural sizing policy. Consider the system summarized in Fig. 1, which shows a loading distribution in blue and a strength distribution in brown. The x-axis shows stress (units are not important for this relative comparison) and the y-axis shows probability density. The values have been chosen such that the A-basis, 0.01 percentile strength is the same as the 3-sigma limit load, so the Margin of Safety as expressed in Equation 2 is exactly zero (the minimum that satisfies the structural policy).

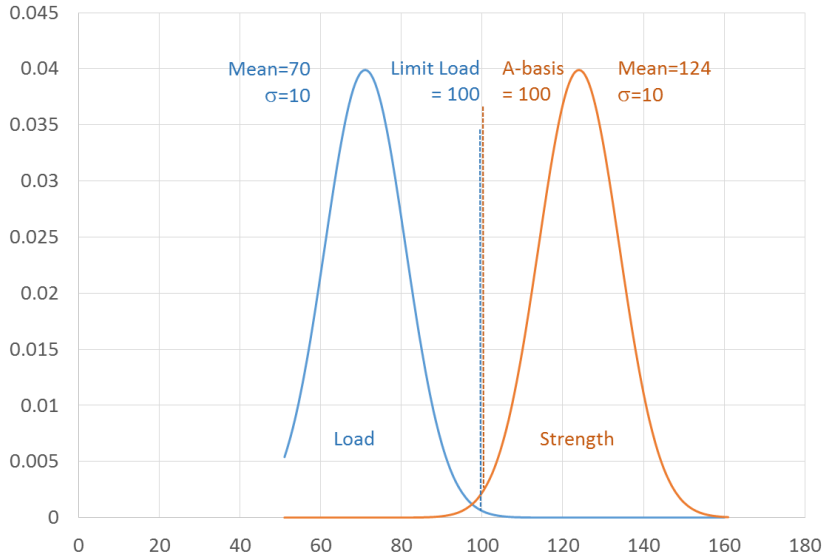

Figure 1. The relationship between strength and load for a margin of safety against yield, for which Factor of Safety = 1.

Failure occurs when applied load exceeds strength. The total likelihood of failure is the sum of likelihoods for each load level as shown in Equation 3.

$$P(failure) = \sum_{-\infty}^{\infty} PDF_{load}(i)dx(i) \cdot CDF_{strength}(-\infty \rightarrow x(i)) \tag{3}$$

For this system, the total probability of failure is 7.72e-5, or close to 1/13,000.

Now consider a similar case, with the same strength and the same limit load (and therefore the same margin of safety). Only the distribution of possible loads is changed: the mean is higher (85) and the variance is lower (5). Here the total probability of failure is 2.86e-4 or close to 1/3,500. Satisfying the same margin policy, the reliability is reduced by a factor close to 4, just by changing the distribution of possible loads. If the underlying loads distribution is unknown during design, then the linkage between design policy and reliability is also unknown. The inset in Fig. 2 shows what is happening, using a load level of 96 as an example. The probability of strength being lower than 96 is the same for both cases, but the probability of the load being 96 is about 4 times higher for the second load distribution than for the first.

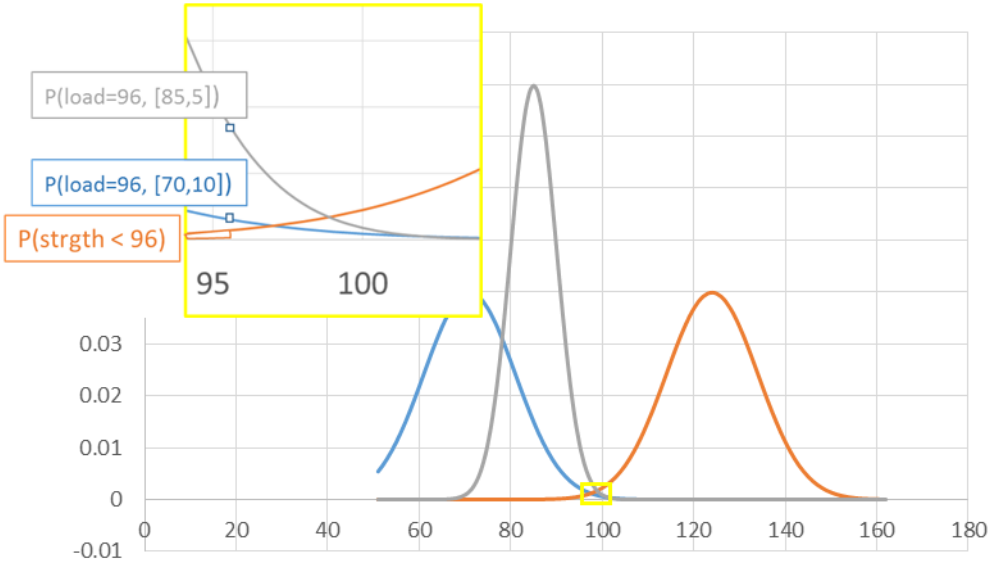

Figure 2. The variance in applied load affects structural reliability, despite a constant margin of safety

A similar example is provided for ultimate load and ultimate strength. The load distributions are unchanged from Fig. 1, except that an additional distribution is introduced, with mean load of 10 and standard deviation of 30. The variance of the strength distribution is maintained, but the mean strength is increased such that an A-basis allowable of 140 is produced. In this manner, with a Factor of Safety of 1.4 on limit load, the ultimate load is equal to the A-basis ultimate strength, and the Margin of Safety is again zero (the minimum that satisfies the structural policy).

Fig. 3 shows that the primary effect of the Factor of Safety is to increase separation between the Load and Strength distributions. Any intersection between them occurs at much lower likelihood than for the un-factored cases. Table 1 shows that ultimate failure probability (FoS = 1.4) for the (70,10) load distribution is a million times lower than limit failure (FoS = 1.0) probability, and for the (85,5) distribution the change is almost 100 million times lower. Such low rates are important for the commercial aircraft industry, which seeks to lower fatality rates to no more than 6.2 per 100 million passengers by 2018 [7]. They are far lower than the levels required for Orion reliability goals.

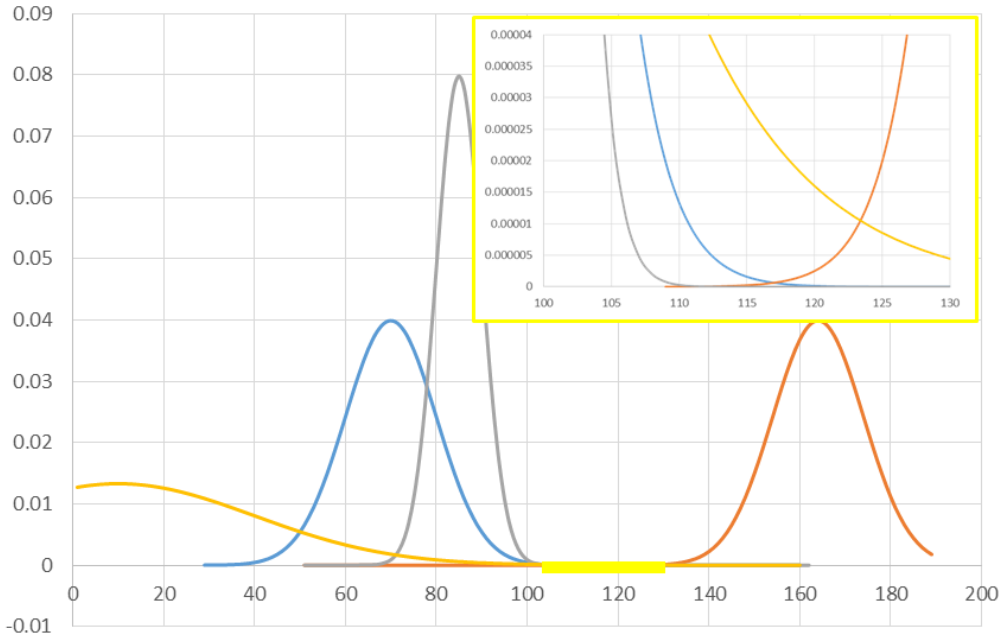

Figure 3. A Factor of Safety separates the tails of the load and strength distributions, and greatly increases structural reliability.

Load			Strength				
Mean	**□**	**Limit**	**Mean**	**□**	**A-basis**	**FoS**	**Failure rate**
70	10	100	124	10	100	1	7.72e-4
85	5	100	124	10	100	1	2.86e-4
70	10	100	164	10	140	1.4	1.88e-11
85	5	100	164	10	140	1.4	1.08e-12
10	30	100	164	10	140	1.4	6.04e-7
85	5	100	144	10	120	1.2	8.29e-8

Table 1. Summary of failure probability for various load cases where M.S. = 0.0.

The inset in Fig. 3 shows that the low mean and high variance load distribution now has a much larger overlap with the strength distribution, and therefore the failure probability is higher. The reliability reversal between the (85,5) and (70,10) load cases occurs because the Factor of Safety is applied both to the mean load and to the variance, so the number of standard deviations between limit load and A-basis allowable is larger when the mean load is large. The (10,30) distribution adds only 1.33 standard deviations, while the (85,5) distribution adds 8.

The final example included in Table 1 considers the (85,5) load distribution with a Factor of Safety of only 1.2. The failure probability is an order of magnitude better than that for the (10,30) distribution with a Factor of Safety of 1.4. This reinforces the point that the structural policy does not guarantee a particular level of reliability. It is possible to adjust the policy and still deliver adequate structural reliability, tailored to the risk posture of a specific program.

III. Probabilistic Risk Assessment of Structural Failure Due Avcoat Cracks for EFT-1 Flight Rationale

The In 2013-2014 as-built hardware testing of the Orion EFT-1 heatshield showed considerably less strength than that achieved in test panels used to develop the design strength allowables. In addition, fabrication cracking in the Avcoat honeycomb seams meant that seam strength was unknown. Given the EFT-1 heatshield fabrication issues, specifically the unknown strength of Avcoat spanning honeycomb seams, the Orion Program could not predict positive Avcoat margins of safety for the EFT-1 flight. A waiver to the Orion structural design policy was written and backed up with a simple PRA considering three incremental failures: Avcoat fracture, subsequent entry

gas penetration and structural overheating, and then structural failure due to the heat-weakened condition. Each of these contributions is considered in turn with an explanation of how each input parametr's statistical distribution was modeled.

A. Fracture of Thermal Protection Material

The methodology for predicting fracture likelihood is the same as that in Section 2, but the load and strength distributions were derived from actual Orion Avcoat material testing and the Orion mission loads. Because multiple loads contributors were in play, the work used a Monte Carlo simulation instead of closed form solutions. The convergence behavior of the Monte Carlo scheme was checked against closed form solutions for the simple cases presented earlier. Convergence to the closed form method was typically found at about 5,000 iterations but the more complex cases here are run to 1,000,000 iterations to assure convergence, since execution time is very small.

Since Avcoat is a composite material, there is no yield behavior and failure probability is only assessed using ultimate strength data form the material test program. Loads are not factored, but model uncertainty factors are used to define the load distributions. This is consistent with the definition of limit load provided above: model uncertainty must be included before a Factor of Safety is applied.

Ablator strength, σ_{ult} is taken directly from material test data at a range of temperatures. A dedicated test program was instituted to develop allowables for the Avcoat HC/G thermal protection material, because it is an unusual material for which handbook allowables are not available. Typical distributions for three temperatures are shown in Fig. 4. The variance in material strength is very high, particularly at low temperature. More testing would likely reduce the variance, but it is conservative to apply the distributions that are based on a relatively small sample set. Within the simulation, strength mean and standard deviation are interpolated based on the applied temperature at each Monte Carlo iteration, to account for the significant temperature-dependence of Avcoat strength.

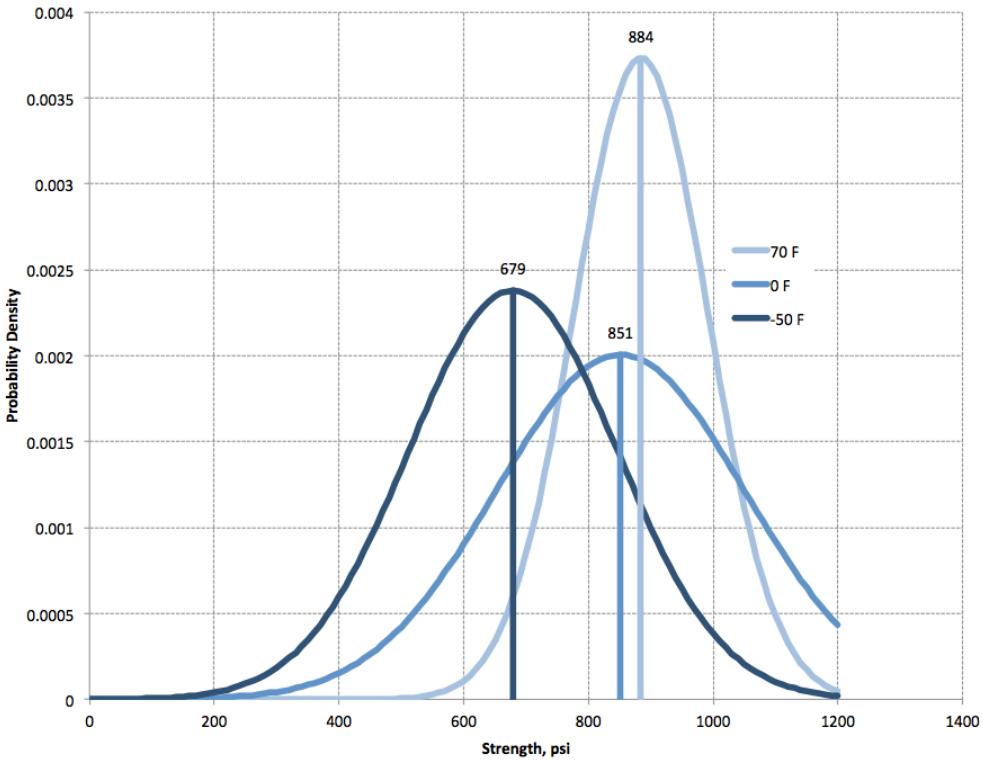

Figure 4: Typical Avcoat Strength Distributions Over a Range of Temperatures

The most severe stresses for the heatshield throughout the mission occur in the entry phase, which is the only loading environment considered here. Ablator stress, σ_{app}, is the combination of mechanical and thermal stresses during entry, given by Equation 4.

$$\sigma_{app} = k_{P_{FEM}} P_{app_{sample}} \frac{E(T_{app_{sample}})}{E(T_{P_{FEM}})} + k_{T_{FEM}} (T_{app_{sample}} - T_{zs_{sample}}) \frac{E(T_{app_{sample}})}{E(T_{T_{FEM}})} \tag{4}$$

The entry pressure and thermal gradient stresses are combined at a single location in the ablator, and σ_{app} is computed at each *sample* within a Monte Carlo simulation. The stress distribution is found by dispersing uncertainties in pressure and temperature.

The substructure is a composite skin over titanium skeleton, so in-plane tensile stresses in the ablator, which are relevant for crack formation, are generated where the skin bends over the stringers due to entry aerodynamic pressure. Entry pressure statistics come from a Monte Carlo trajectory population provided by the Orion Guidance, Navigation and Control (GN&C) team. A typical case is a Gaussian peak pressure distribution with a Coefficient of Variance (CoV) of 5%.

Thermal stresses are primarily generated by the difference in Coefficient of Thermal Expansion (CTE) between ablator and substrate and the change in temperature from the zero stress state established during the final manufacturing cure to the operating temperature during the mission. Both the zero-stress temperature, T_{zs} of the ablator-substrate system and the applied mission temperature, T_{app}, are dispersed and sampled independently. T_{app} distributions come from on-orbit thermal modeling and T_{zs} distributions come from system test data. When peak entry pressure is near the beginning of the entry trajectory, and cold temperatures relative to the zero-stress temperature dominate stress, the entry interface temperature can be used in equation 4. In other cases, one must use the ablator system temperature at the time of peak pressure. This work conservatively used the coldest predicted entry interface temperature of 30° F as the mean and a standard deviation of 10° F based on the range of input parameters in the Passive Thermal Control (PTC) simulations. The zero-stress temperature, T_{zs}, distribution is a Gaussian with a mean of 170° F with a standard deviation of 10° F.

Because the computational expense of running Finite Element Model (FEM) analyses in-line with a Monte Carlo simulation is prohibitive, a (FEM)-generated factor translates the applied pressure and temperature into stress. This translation assumes the stresses are linear with respect to both load level and Young's Modulus, E. Both k_{PFEM} and k_{TFEM} are found from single FEM stress solutions for given pressure and temperature loads and held constant. Temperature dependent ablator modulus, E is looked up from material property data at each iteration as a function of the sampled applied temperature, T_{app}. The ratios of pressure, temperature and modulus between the values sampled for each case and the values used in the FEM case are then used to scale the sample stresses with respect to the FEM stresses.

Several variational studies were conducted, and are summarized in Table 2. The first case is considered nominal, with a pressure load of 5.1 psi and standard deviation of 0.26 psi. Note that these are pressures applied normal to the heatshield surface, which induce stresses in the Avcoat that can be hundreds of psi. The zero stress temperature is 170 F, and the mean operating temperature is 30 F, so the change in temperature that drives Avcoat stresses is 140 F, with a standard deviation of 10 F. If a normal distribution is fit to the set of sampled load cases, the combined loading generates a mean stress of 447 psi and standard deviation of 54 psi. The probability of failure, from a million Monte Carlo runs, falls in a range from 1/80 to 1/140 as load distribution assumptions are varied. Despite large negative margins calculated from the structural design policy, it is far from certain that cracks would be created in a mission.

Case	Pf	MS
dT: 170F -> 30F, σ = 10F Pressure: μ = 5.1 psi, σ = 0.26 psi Stress: μ = 447 psi, σ = 54 psi Strength: μ=*f*(T)=862 psi, σ=*f*(T)=161 psi	Basic: 1 in [80 – 140]	A: -0.65 B: -0.24
dT: 200F -> 30F, σ = 10F Pressure: μ = 5.1 psi, σ = 0.26 psi Stress: μ = 513 psi, σ = 57 psi Strength: μ=*f*(T)=862 psi, σ=*f*(T)=161 psi	Basic: 1 in [35 – 45]	A: -0.69 B: -0.34
dT: 170F -> 30F, σ = 10F Pressure: μ = 5.1 psi, σ = 0.26 psi Stress: μ = 447 psi, σ = 54 psi Strength: μ=*f*(T)=862 psi, σ=*f*(70)=113 psi	Basic: 1 in [2,100 – 2,400]	A: -0.32 B: -0.04
dT: 170F -> 30F, σ = 10F Pressure: μ = 0 psi, σ = 0 psi Stress: μ = 313 psi, σ = 35 psi Strength: μ=*f*(T)=862 psi, σ=*f*(T)=161 psi	Basic: 1 in [1,200 - 2,100]	A: -0.50 B: +0.05

Table 2. The effect of different modeling assumptions on predicted probability of crack formation.

The second case modifies only the assumed zero stress temperature. Increasing this temperature to 200 F increases the thermal stress induced in the Avcoat, and the mean combined stress increases by 15%. The margin of safety, already highly negative, gets slightly worse, but the probability of failure doubles, to a range of 1/35 to 1/45.

The third case restores the zero stress temperature to its original value, and adjusts the assumed strength distribution, by assuming that the variance observed in tests at 70F would apply at all temperatures. This eliminates the effect of large variance in tests conducted at -50F, and significantly increases the A-basis allowable. The probability of failure is greatly reduced, to below 1/2,000 while the margin of safety remains negative.

The final case differs from the original by eliminating pressure loading entirely, so the stress is entirely due to thermal loading. The margin of safety against A-basis allowables is still -0.5, and the probability of failure is between 1/1,200 and 1/2,100.

These results point to a number of possibilities for improving the margin of safety for Avcoat. Indeed, independent of the current work, the program ended up being able to show positive margin against B-basis allowables for the EFT-1 mission in all areas except the honeycomb seams. One key change was to increase the minimum operating temperature, which positively affects both the thermal load and the stiffness of the material to which the load is applied. Furthermore, the strength variance was reduced when the behavior below 0 F was excluded, because it is not relevant for the updated operating conditions.

By similar reasoning, the Case 1 results are conservative relative to the operating environment ultimately defined for the EFT-1 mission. Nevertheless the lower bound of that probability range is used for Term 1 of Equation 1 in the upcoming LOM calculation.

B. Bondline Overheating

The second term of Equation 1 is concerned with the likelihood of bondline overheating given that a crack has been created. The nominal bondline temperature is calculated through 1-D thermal analysis, based on the heating rate history supplied by aerothermal analysis, and on the material response properties of Avcoat. For calculation of the nominal temperature, nominal values are assumed for all input parameters. Variations associated with the heating profile, due to uncertainty in trajectory and in aerothermodynamics, and with the mechanical and chemical response of the material all affect the variance of bondline temperature around the nominal case. The influence of a crack is one additional term to be considered in Equation 5.

$$T_{final} = T_{nominal} + \Delta T_{trajectory} + \Delta T_{aerothermal} + \Delta T_{material} + \Delta T_{recession} + \Delta T_{crack} \quad (5)$$

All of the variances are shown as increments added to the mean. Several of the terms are symmetric about the mean, so they may have a negative value for a particular sample. The influence of a crack is biased in the simulation, such that it will only increase bondline temperature.

$\Delta T_{trajectory}$ is found from thermal analyses at the mean and 3-sigma high heat load trajectory within a population of 3,000 trajectories. The hottest bond line temperature at any Heat Shield location was 238 F for the nominal trajectory, and 246 F at the 3-sigma high heat load trajectory. $T_{nominal}$ is then 238 F and the $\Delta T_{trajectory}$ dispersion is a Gaussian with a mean of 0 F and a standard deviation of (246-238)/3 = 2.37 F.

The Aerothermal community provides heating augmentation factors to account for environment modeling uncertainties. These factors were assumed to cover a 3-sigma uncertainty distribution. $\Delta T_{aerothermal}$ is found by finding the largest bond line temperature difference at any Heat Shield location with and without these factors applied. The largest difference was 28 F so $\Delta T_{aerothermal}$ was set with a distribution mean of 0 F and a standard deviation of 28/3 = 9.3 F.

The effect of material property uncertainties was found from an unpublished study performed at NASA JSC in 2011. That work was a Monte Carlo analysis, in which material property inputs to a thermal model were varied according to tested and assumed property data. The study produced a bond line temperature distribution with a 67 F standard deviation. The $\Delta T_{materal}$ distribution is then normal with a mean of 0 F and standard deviation of 67 F.

$\Delta T_{recession}$ can be derived directly from test-to-model recession comparisons over a set of arc jet ablator tests. However, due to ground-to-flight traceability concerns, the work here took a simpler approach and treated recession uncertainty as a reduction in initial thickness based on the thermal margin policy used in design. Since the margin policy used to design Avcoat thickness applied a minimum of 10% extra thickness to account for recession modeling uncertainty, which was assumed to be a 3-sigma increment, the standard deviation for reduction of initial thickness is 0.033.

A distribution with a mean of 1 and standard deviation of 0.033 was used to sample a curve of bondline temperature ratio as a function of reduced initial thickness ratio. Fig. 5 illustrates the model. The sampling process selects an initial thickness ratio, and uses the function in Fig. 5 to assign a temperature ratio that is applied to the temperature constructed for the sample due to all the other variance contributions, as shown in Equation 6. Because recession is an energy consuming process, it is excessively conservative to treat the effect of recession uncertainty as reduced thickness from the start of the heating pulse. To account for this, the difference between 1.0 and the sampled thickness ratio was divided by half before looking up the corresponding temperature ratio. For example, a sample of 0.8 resulted in a thickness ratio of 0.9 being used to look up the temperature ratio. The resulting temperature ratio was then conservatively applied to the stacked trajectory, aerothermal, and material effects as shown in Equation 6.

$$\Delta T_{recession} = (T_{nominal} + \Delta T_{trajectory} + \Delta T_{aerothermal} + \Delta T_{material}) \cdot \frac{T}{T_{initial}} \quad (6)$$

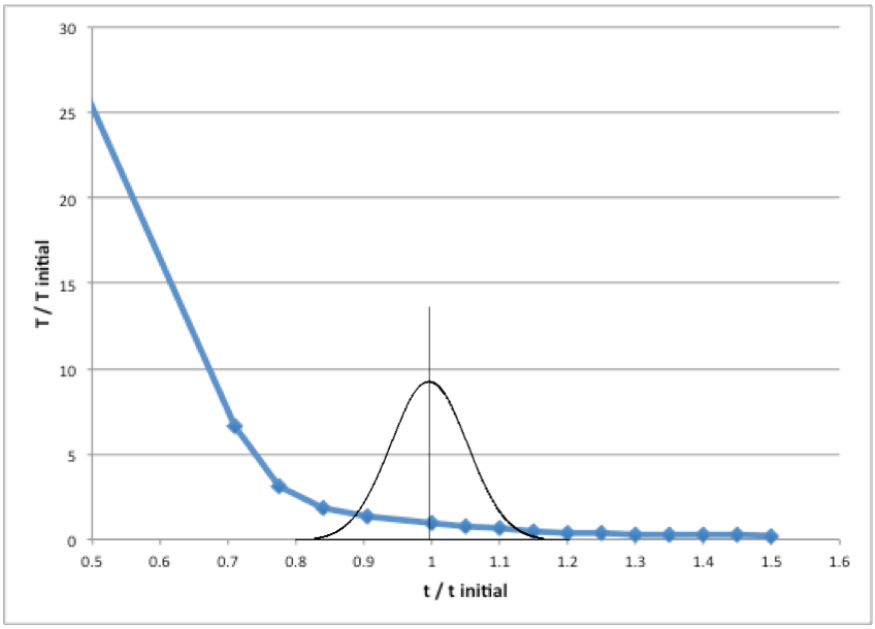

Figure 5: Bond Line Temperature Ratio as a Function of Initial Thickness Ratio

Finally, ΔT_{crack} is derived from arc jet testing of cracked Avcoat samples that were subjected to heating profiles more severe than what is anticipated for the EFT-1 mission. A post-test photograph of a sectioned test article is shown in Fig. 6. There is clearly greater char depth in the neighborhood of the crack, but there is still virgin material above the bondline.

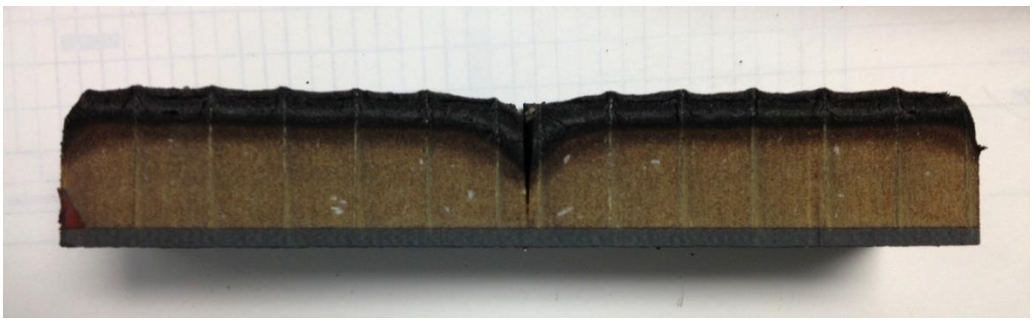

Figure 6: Post-Test Cracked Avcoat Arc Jet Sample

The cracked Avcoat arc jet models had temperature sensors placed directly below the crack and off to the side in the un-affected area. Over 13 tests across the range of expected crack widths, the mean peak temperature difference between the two temperature measurements was 15.6 F, with a standard deviation of 12.8 F. ΔT_{crack} was set to a distribution with exactly those parameters, except that the lower side of the distribution is truncated at zero, so that the crack can never have the effect of reducing bondline heating.

The influence of each of the contributors to variance in bondline temperature is shown in Fig. 7. It is clear that the effect of material property variability dominates all other contributions to elevated bondline temperature. Introduction of a crack does shift the distribution a little to the right, but the impact of the crack is clearly modest. If a Gaussian distribution is fit to the temperatures predicted by Monte Carlo sampling, the mean is increased from 238 F to 254 F, and the standard deviation is 70 F (which is a modest increase from the 67 F for material property variation alone). The allowable temperature of 500 F sits at the 99.95%, or 3.3-sigma likelihood. With the influence of cracks included, the likelihood of the bondline exceeding 500 F in Monte Carlo simulations ranged from 1/2,000 to 1/3,000. Without cracks, the range was 1/4,500 to 1/5,500. The influence of cracks roughly doubles the likelihood of exceeding the bondline temperature allowable.

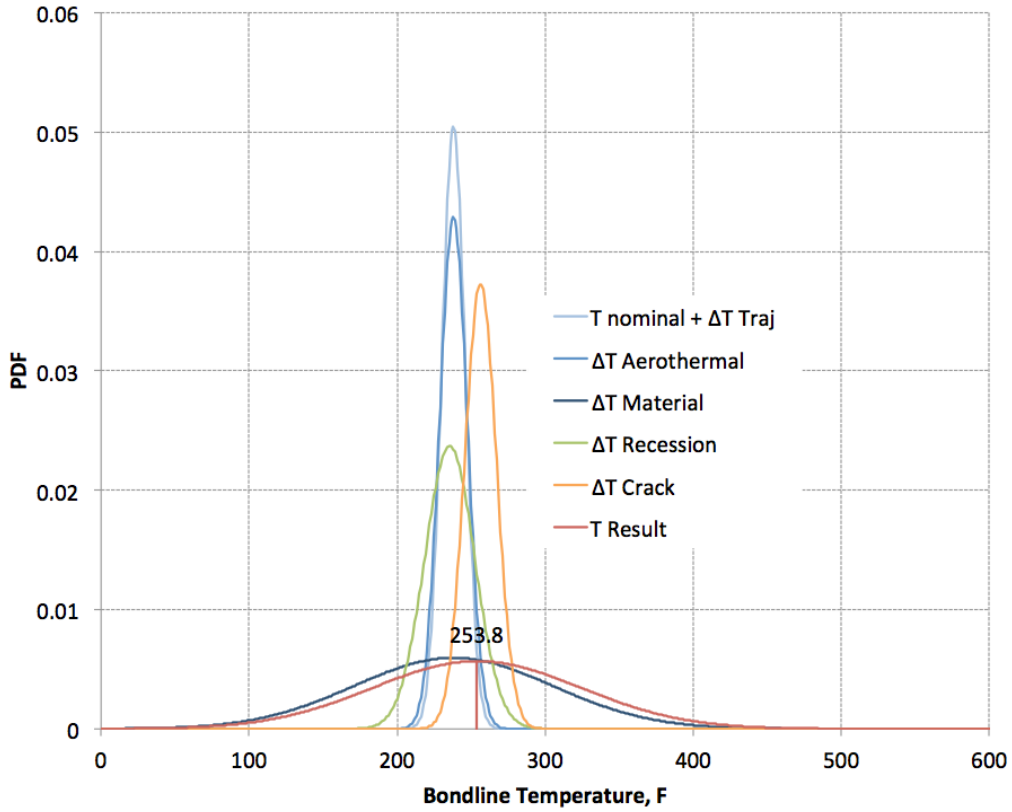

Figure 7: Bondline Temperature Results

C. Loss of Vehicle

The third term of Equation 1 is concerned with the probability of structural failure given a bondline over temperature. The first two terms yield a likelihood of bondline temperatures over 500 F as 1/160,000 (1/80 for crack creation and 1/2,000 for bondline exceeding allowable temperature), which is much lower than the 1/5,300 allocation for TPS and therefore provides adequate flight rationale. Nevertheless, some evidence is provided to show that the probability of structural failure even in the case of an over temperature is substantially lower than 1.

Temperature	Cases > 500F out of 1M	% of Cases
500	484	0.05%
510	318	0.03%
520	208	0.02%
530	132	0.01%
540	84	0.01%
550	46	0.00%
560	35	0.00%
570	19	0.00%
580	9	0.00%
590	3	0.00%
600	2	0.00%
665	0	0.00%

Table 3. Number of cases that exceed allowable temperature, for 10 F increments of exceedance.

The key driver is that structural strength decays slowly with temperature, and the magnitude of most temperature exceedances is modest. Table 3 indicates that the probability of reaching 550 F is just 1/10 of the probability of reaching 501 F. Only 2 cases out of the million samples in this Monte Carlo run exceed the allowable temperature by 100 F. If strength is reduced by 30% due to such a temperature increase, the A-basis strength will still be similar to limit load (effectively the reduction in strength would cancel the Factor of Safety of 1.4). Section 2 showed that the probability of failure for such a situation is better than 1/10,000. It is likely that a basic model for strength reduction as a function of temperature, driven with predicted bondline temperatures from the previous subsection, will show very low probability of structural failure.

IV. Conclusions

It is very difficult to show positive structural margin against cracks for an Orion heatshield using Avcoat HC/G as the thermal protection material with Orion stress policies. Although most of the heatshield was ultimately cleared for the EFT-1 mission, the modeling relied on benign cold soak temperatures that would not be acceptable for a long duration mission.

Despite the lack of positive structural margins, it is possible to show that the probability of catastrophic consequence of cracking is acceptably small. This conclusion relies on experimental evidence from arc jet testing that the crack causes a very modest increase in the temperature at the bondline. The conclusion also relies on conservative judgments about load uncertainty and other parameters to define all of the necessary statistics.

More detailed models would further improve the predicted reliability. Variance in the thermal response model is dominated by the effects of material property uncertainty. Refinement of this part of the model is expected to significantly improve the predicted probability of bondline temperature exceedance. Modeling of the effect of bondline temperature on the strength of primary structure would have an even larger beneficial effect on predicted probability of LOM for this failure mode.

The relationship between stress analysis policy and probability of failure is not commonly appreciated. Some simple examples were provided to demonstrate the effect of variance in strength and loading on the failure probability associated with a fixed structural design policy. There is an opportunity to use probabilistic assessment to tailor policies for specific applications.

The demands of structural and thermal sizing policies are not well balanced. The structural policy delivers "failure" rates that are far better than 1e-6 (and for reasonable levels of variance the ultimate failure rates are closer to 1e-10), while the thermal policy delivers a "failure" rate, for uncracked material, of around 1/5,000. Adjustment of the thermal policy to address the probabilistic implications is warranted.

Acknowledgments

The authors wish to thank Brian Remark of JSC for material property study results, Sam Preece and Robby Aungst of Lockheed Martin for their Finite Element Modeling support, and Scott Durrant of Lockheed Martin for the thermal effect of initial thickness model.

References

[1]NASA NPR 8000.4a, NASA Risk Management Procedural Requirements, http://nodis3.gsfc.nasa.gov/displayDir.cfm?Internal_ID=N_PR_8000_004A_

[2]Vander Kam, J., Howard A., Gage, P., Schiermeier, J., The Devil's In The Tails – Reliability Prediction Methodologies for the Orion Heatshield, AIAA 2011-422

[3]NASA STD 5001B, Structural Design and Test Factors of Safety for Spaceflight Hardware https://standards.nasa.gov/standard/nasa/nasa-std-5001

[4]NASA STD 5002, Load Analyses of Spacecraft and Payloads, https://standards.nasa.gov/standard/nasa/nasa-std-5002

[5]NASA STD 6016 Standard Materials and Processes Requirements for Spacecraft https://standards.nasa.gov/standard/nasa/nasa-std-6016

[6]Federal Aviation Administration Destination 2025 https://www.faa.gov/about/plans_reports/media/Destination2025.pdf